Available online at www.sciencedirect.com
SCIENCE DIRECT®
Journal of Power Sources 129 (2004) 193–204
JOURNAL OF POWER SOURCES
www.elsevier.com/locate/jpowsour

The evolution of the performance of alkaline fuel cells with circulating electrolyte

P. Gouérec*, L. Poletto, J. Denizot, E. Sanchez-Cortezon, J.H. Miners

Eident Energy, Independent Power Technologies SAS, Savoie TechnoLac, BP 311, 73375 Le Bourget du Lac, France

Received 24 July 2003; accepted 15 November 2003

Abstract

The most recent information is presented concerning the development of the alkaline fuel cell (AFC) with circulating aqueous electrolyte technology at Eident Energy (EE). The latest version of this commercially sold sub-stack or "module" results in improved performance (400–430 to 590 W at 4 V and 51% total efficiency (η) versus LHV, i.e. from 100 to 137 mA cm^{-2} at 0.67 V per cell) and durability (2500 h expected with 10% decrease in power when operating at constant nominal current). The catalyst content in the module is also reduced from 1.2 to 0.5–0.6 mg cm^{-2}. These improvements were achieved via an optimisation the porosity of the electrodes in order to obtain greater air diffusion inside the electrode.

The authors also present the results of experiments that determine the origin of the performance loss of the AFC module over time. In contrast to much of the literature, the results do not support the irreversible corrosion of materials due to the oxygen reduction reaction. Indeed, over the investigated working period (i.e. ca. 1500–2000 h), the degradation of the performance was attributed to a slow and constant physical flooding due to imperfections in the wet proofing coating. Based on these facts, strategies are proposed to slow, avoid and even reverse to this flooding.

Keywords: Alkaline fuel cells; Ageing; Oxygen reduction reaction; Low Pt loading

1. Introduction

Although several companies are starting to commercialize small PEMFC stacks, low temperature fuel cells still suffer from low durability (<5000 h) and high costs (materials cost > 1000 €/*kW*). These two factors prevent their commercialisation. It is for this reason that there has been, in recent years, the reemergence of interest in circulating aqueous alkaline fuel cells (AFC) [1,2]. AFCs appear suitable and attractive for a wide range of applications due to the robustness of their stacks and systems and their potential for low cost [3]. In recent articles, McLean et al. [5] and Kordesch et al. [4] review AFC technology and examine its economic potential in direct comparison to PEMFC and conclude to the competitive position of AFCs versus other low temperature fuel cells.

The inherent performance and cost advantages of a fuel cell with an alkaline electrolyte may be ascribed to two key factors. The higher kinetics for the oxygen reduction reaction (ORR) in alkaline over acidic media permits the use of a lower quantity of precious metals for a given overpotential. This results in a greater efficiency for the AFC when compared to the PEM as well as a large margin for the cost reduction. Secondly the alkaline media (i.e. KOH) is less aggressive/corrosive to metal and carbon than acid. The less-corrosive nature of an alkaline environment ensures a potential greater longevity and allows the implementation of non-noble catalysts, both for the cathode and the anode [6,7]. Low cost structural materials such as nickel current collectors and plastic composite frames are also stable in contact with KOH.

The durability of the low temperature fuel cells (AFC and PEMFC) is also a critical issue to overcome. The targets for fuel cells durability required for mobile and stationary applications have been determined by the US Department of Energy to be 5000 and 40,000 working hours, respectively.

1.1. Electrolyte leaking and carbon dioxide poisoning

The fuel cell literature quotes a number of inhibitors to the terrestrial application of AFC using air. Problems include electrolyte (KOH) leaking and CO_2 poisoning. These "show stopping" problems have been successfully overcome over the past 20 years.

* Corresponding author.
E-mail address: pascal.gouerec@laposte.net (P. Gouérec).

0378-7753/$ – see front matter © 2003 Elsevier B.V. All rights reserved.
doi:10.1016/j.jpowsour.2003.11.032

1.1.1. Electrolyte leaking

KOH leaking, a key problem in filter-pressed stacks, has been solved by developing a stack manufacturing process in which electrodes are framed via the injection moulding of a plastic composite directly onto an electrode, followed by the friction welding of the electrodes to form a sub-stack. This results in a monoblock of plastic, in which there are no holes or cracks through which KOH can leak. There is always some small quantity of KOH, which may creep though the electrodes into the gas chambers (up to 15 ml h^{-1}/kW of stack). This liquid is collected at the exit of the stack and dripped directly back into the electrolyte reservoir [8].

1.1.2. CO_2 poisoning

The 300–350 ppm of CO_2 contained naturally in air has also been responsible for increased performance degradation in some AFCs [9]. On contact with CO_2, KOH reacts to form potassium carbonate (K_2CO_3), thereby reducing the OH^- concentration. If a significant reduction in the concentration of OH^- ions occurs, one observes a reduction in the ionic-conductivity of the electrolyte, as well as an increase of the electrolyte viscosity. This also results in interference with electrode kinetics and diffusion properties. The reduction of OH^- concentration is critical in a non-replaceable non-circulating (matrix) AFC in which there is only a small volume of KOH present. This contrasts with AFC with circulating electrolyte where 10–100 times more KOH is present (i.e. 1–2 l of KOH per kW of stack). The use of a KOH circulating electrolyte increases the tolerance to CO_2 and one has the possibility to replace/add extra KOH should the OH^- concentration become too low. It should be noted that 1 l of 6.6 M KOH costs between 1 and 3 €, and contains enough ions to react away 100% of the CO_2 contained in a volume of 250 N m^3 of air. This is the volume of air necessary to produce 150 kWh of electricity (at 53% electrochemical efficiency (E.Eff.) versus LHV and 1 time the airflow stoichiometry). The cost of scrubbing the air via reaction with KOH in this manner is 0.7–2 cents/kWh.

At high concentration (7.9 M at 20 °C, and 9.67 M at 70 °C [10]), K_2CO_3 precipitates and may block gases pores and thus limit the gas diffusion inside the catalytic layer to the active sites. It should be noted that to achieve this high concentration of K_2CO_3 one would require an initial local concentration of 15.8–19.3 M KOH, i.e. an increase of the local concentration of KOH by 2.4 and 2.9 times the KOH bulk concentration (6.6 M), at 20 and 70 °C, respectively. At these high concentrations one already stands a high risk of KOH precipitation, resulting in a similar pore block and limitation of the gas diffusion. KOH precipitates at 20.3 and 27.1 M at 20 and 70 °C, respectively. Precipitation may be avoided by ensuring a good liquid transport in the cathode. This reduces KOH and K_2CO_3 concentration gradients and inhibits the build up of the high local concentrations K_2CO_3 and KOH to levels at which precipitation occurs. This is achieved via an appropriate modification of the cathode pore structure. This prevents the precipitation of K_2CO_3 in the gas pores to the point that one can eliminate the need for CO_2 scrubbers [11]. Indeed, Gülzow reports AFC electrodes which exhibit stable performance over 3500 h at 0.15 A cm^{-2} when operated with 5% CO_2 in O_2 (150 times the CO_2 concentration in air!) [11]. Performance remained constant even when the total carbonate concentration in the electrolyte was in excess of 3.3 M.

The most common way to eliminate the negative influence of CO_2 is simply to remove it. This is achieved using commercial CO_2 scrubbers to scrub the air. Chemical scrubbers (i.e. soda lime) or regenerative scrubbers (which function on the principles of pressure-swing adsorption, temperature-swing-absorption, and the steam-regeneration of amines [2]) are available and can reduce the concentration of CO_2 to 5 and 30 ppm, respectively, with minimal power consumption and cost. McLean et al. calculate the cost of a soda line scrubber as 0.2–2.6 cents/kWh [5].

1.2. Performance

As it is shown by Lindstrom [12] and confirmed elsewhere [13], AFC systems demonstrate higher performances in respect to PEM when operating under identical conditions (i.e. the same gas pressures and operating temperature). Pressurised AFCs remain the system of choice for manned-space applications having proven their high power density, reliability and robustness. These fuel cells, which operate on hydrogen and pure oxygen, provide high current densities at high fuel cell efficiencies.

Independent Power Technologies Ltd. has recently developed a 6.0 kW net ambient system incorporating the V1.0 Eident Energy (EE) stack [2]. Operating at >47% total efficiency versus LHV, it has a power density of 45 kg/kW and 96 l/kW. The integration of the most recent V1.1 EE stack into same system is projected to achieve 8.3 kW net with a power density of 30 kg/kW and 64 l/kW [2,14]. A critical source for a comparison of AFC versus other low temperature technologies can be also found in the latest surveys of the AFC technology [5].

The intrinsic advantage of using alkaline over acidic media is due to the greater kinetics for the oxygen reduction reaction (ORR) [7,15]. The practical consequence of the greater kinetics is that, for a given platinum utilisation/loading and a given set of operating conditions (current density, temperature, gas pressures, gas stoichiometry), an AFC is capable of higher electrochemical efficiencies at a given current/power density compared to fuel cells with an acid electrolyte (i.e. PAFC and PEMFC). Not only does the faster kinetics for the ORR allow for lower loadings of precious catalysts to be used, but it also allows the use of non-noble and less costly catalysts [7]. As in acidic media, the hydrogen oxidation reaction (HOR) in alkaline media does not suffer from large losses. Indeed the kinetics of the HOR is several orders of magnitudes larger than for the ORR (ca. 10^{-3} versus 10^{-9} to 10^{-11} A cm^{-2}) when appropriate catalysts are chosen [7,16].

The ORR is always the main source of electrochemical losses limiting the performance of the hydrogen-air fuel cell. As an example, in an EE V1.1 module, at nominal power, the efficiency losses due to low ORR kinetics represent 30% of the total module losses whereas the 68% of the total module losses is related to the cathode [17]. The fuel cell efficiency is critical in achieving an economically viable cost of the electricity generated. The cost of the electricity generated (given in €/kWh of operation) is comprised of the direct cost of the system, plus the cost of the fuel (plus the cost of maintenance, installation, etc.). The importance of fuel cell efficiency can be judged by the following statement: the fuel cost represents 96% of the total cost of the electricity produced over a 5000 h working period at 51% total efficiency versus LHV when calculating using the current cost of € 3 per N m^3 H_2 and the bill of materials (BOM) cost of an EE V1.1 module (equal to € 454/kW when the materials are acquired at prices quoted end May 2003 in a volume equivalent for a production run of 25 kW). When using the predictions of future hydrogen costs given by the US DOE (i.e. € 0.2 per N m^3), the cost of the fuel will represent 62% of total cost of the produced electricity [14].

1.3. System lifetime and stack durability

The current durability of the low temperature fuel cells system is a key factor in preventing their commercial application. As a general remark, comparing the durability of one type of fuel cell to another is made complicated due to the absence of a strong definition of lifetime. This definition is outside the scope of most performance test codes e.g. those recently published by the ASME [18]. Durability for AFCs systems has been established many times to be in excess of 5–8000 h [19,20] and in some cases to even reach 15–20,000 h [21,22]. For the medium–high temperature fuel cells impressive durability has been demonstrated for field applications of the PAFC 250 kW (PC-25 from IFC) with an excess of 40,000 h reported. This meets the DOE requirements for stationary applications. Nowadays, the warranted lifetime for field use for PEMFC integrated system does not generally exceed 2000–3000 h according to the constructors' specifications [1]. Similar values are also reported for AFC systems. Interestingly one can argue that, since the chemical and thermal conditions are less corrosive and aggressive to metals and carbons in AFC (30 wt.% KOH, 70 °C) than in PAFC (100 wt.% H_3PO_4, 240 °C) [23], the 50,000 continuous working hours, achieved in PAFC could be targeted as a feasible goal for AFC.

According to several authors, not enough was done on to find out the reasons for the decay of AFCs, simply because they worked satisfactorily for space applications where the requirements are high power and high reliability [3]. To our knowledge, the latest survey of the causes of the degradation in AFCs is more than 10 years old and was published by Kordesch and co-workers in 1992 [19].

System lifetime. If one is to discuss the commercial viability of a fuel cell application, one should consider the robustness and longevity of an integrated system. This is represented by the value of the 'mean time between failure' (MTBF) of the system. The MTBF of a system is determined by two factors: MTBF of system peripheral components (i.e. non-stack components) and MTBF of the stack. The stack failures can be split into two types, the long and gradual degradation of stack performance over time ("stack durability") and catastrophic failure.

A previous, more complicated and more demanding system design developed during the late 1980s by the company Elenco Nv., resulted in a mean time between failure of the peripheral of 2500 h, and a mean time between failures of the stacks of 1750 h [25]. A schematic of a 5–10 kW EE fuel cell system is given in Ref. [8]. The lower number and relative simplicity of system components, in an AFC system inherently results in a long MTBF of system peripheral components. Catastrophic failure rate is inherently low in an AFC stack due to its relative insensitivity to humidity and temperature. The broad range of operating conditions combined with the use of a circulating, inorganic, replaceable liquid electrolyte results in a robust stack.

Catastrophic failure of a cell will also inhibit the operation of all other cells in the stack it is connected to in series. The monopolar module configuration developed by EE allows cells to be connected in series and parallel. EE 24-cell modules are connected electrically with 6 cells in series and 4 in parallel. If a cell suffers a catastrophic failure, the cell group can be disconnected and the rest of the stack can continue to operate as previously. Cell failure results in a decrease in the power by 1.5% in the 16-module system described above [2,17]. This is in contrast to stacks containing bipolar plates, in which all cells are electrically connected in series: if one cell fails, the whole stack fails. Indeed PEM system design is being considerably adapted to avoid the problems of this catastrophic failure [26].

Furthermore, the circulating electrolyte used in an AFC results in a simple and rapid start-up and shutdown procedures [4] and has the additional advantage of simplifying the water and the heat management [8].

Stack durability: The paper published by Kordesch and co-workers in 1992 related to the causes of the degradation in AFC and emphasised on the loss of performance due to the electrochemical corrosion of the electrodes [19]. The multi-layered, PTFE bonded electrodes discussed by the authors were developed and characterised at the Institute for Hydrogen Systems (HIS). These electrodes were produced via a similar manufacturing approach to that used at EE. They were connected in series in a module via a bipolar configuration. A lifetime over 3500 h at $j = 0.1$ A cm^{-2} in 12N KOH at 65 °C is reported (precious metal loading = 1.5 mg cm^{-2}). In the paper, a degradation of the performance under working conditions is reported to be 10–30 mV/1000 h for the cathode. Recent V1.1 cathodes developed at EE have a lower metal loading of <0.3 mg cm^{-2} and show a

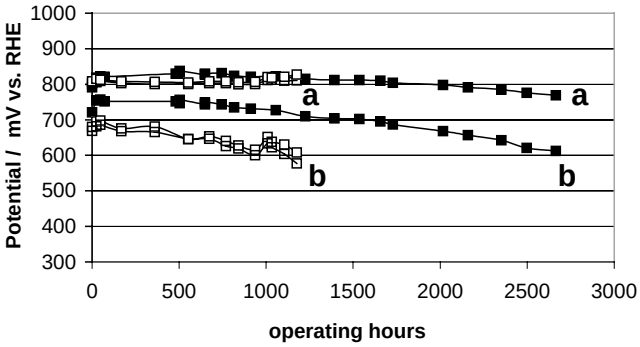

Fig. 1. Evolution of the performance of the V1.0 (□) and the V.1.1 (■) EE cathodes in half-cell configuration at 0.1 A cm^{-2} (a), 0.15 and 0.2 A cm^{-2} for V1.0 and V.1.1 respectively (b).

degradation of 5–10 mV/1000 h over a period of 2800 h at 0.1 A cm^{-2} (Fig. 1). This result also compares favourably with the degradation rate of 17 mV/1000 h achieved with silver based cathodes [11].

Kordesch and co-workers observe a reduction of the electrode surface area and an increase in the wetting of the electrode as a function of hours the electrode is operated [19]. The increased wetting results in a hindrance to the air diffusion inside the catalytic layer, which results in a slow degradation of the electrochemical performance with operating time. The presence of Pt was found to accelerate the rate of corrosion while adding PTFE delayed its rate. They also report the denaturing of the PTFE binder with time, and loss of hydrophobicity of this material.

It is known that highly reactive species, such as HO_2^- [27,28] are by-products of the ORR. Peroxide oxidises carbon and carbon surface groups to form a variety of oxygen-containing surface groups (e.g. carbonyl and carboxylic groups). These polar surface groups reduce the inherent hydrophobicity of the carbon. Carbon combustion and corrosion occurs when these groups desorb from the carbon surface as CO_2/CO, exposing a free carbon site to react with further peroxide [29]. Kordesch and co-workers conclude that the main source of performance degradation was due to the corrosion of the carbon (in this case a Vulcan XC-72-R, a carbon black derived from oil, from the company Cabot Carbon) due to the electro-generation of HO_2^- during the ORR as well as the chemical reaction of the carbon with the KOH.

The carbons ability to decompose the peroxide is determined by its structure (amorphous/graphitic) and the number and type of surface groups present. It follows that modifying the surface properties of the carbon plays an important role towards the stability of the carbon carrier [30]. Thus it was concluded that the improvement in the stability of the carbon materials would be necessary to significantly prolong the lifetime of the air electrode in an AFC [19]. Interestingly, the corrosion of the noble electrocatalyst was neither a lifetime-limiting factor in the cathode nor in the anode [19]. In contrast, Kiros et al. recently discussed the evolution of the anode electrochemical performance. Here, they attributed the decay to be due to morphological changes of the Pt–Pd particles via the sintering under electrochemical load [31,32].

A priori, one must also consider the role of corrosion and contact loss of the electrode with the current collector [19] and the attack of the cell frame [19,22]. However, these parameters appeared to be less critical for the robust AFC technology. Furthermore, one cannot exclude the possible role of the stack assembly steps on the durability of the module. However, given their nature i.e. injection moulding, friction welding, module and stack assemblies this seems unlikely that they would have a large role in the present case.

In the present paper, several aspects related to the improvement of the performance and the durability of the EE AFC module will be addressed by the authors. The cost evaluation will be presented. Moreover, the reasons of the decay of the performance over the first 1500–2000 h under polarisation will be discussed.

2. Experimental

2.1. Electrodes fabrication

A detailed description of the manufacturing process can be found in Ref. [8]. Briefly, the anodes and cathodes are multi-layer gas diffusion electrodes. The active layer of ca. 120 μm thick consists of a mixture of a noble-metal catalyst supported on carbon, PTFE powders and a pore former. The dry powders are mixed together, agglomerated at low temperature and finally rolled at room temperature to form a thin sheet (of ca. 400 μm thick). The gas diffusion layer is of ca. 300 μm thick. It consists of a porous PTFE, and performs the role of a hydrophobic backing layer and hydrophobic layer on the gas side. It is rolled together with the catalytic layer. Finally, the combined layer is pressed into a conductive metal/nickel mesh, which serves both as a current collector and to give the electrode mechanical strength and structural support in the module. As described above, the electrodes are framed with a plastic composite via an injection-moulding technique and the module is assembled via the friction welding of the electrodes together. Additional technical information on the module fabrication and system design and integration is also described in Refs. [2,8].

2.2. Module configuration

The stand-alone module is made of 24 cells connected in series (6 cells)/parallel (4 groups of 6 cells). The surface of a single cell is 16.8 cm × 16.8 cm. Connected in this fashion, a module current of 107.6 A (for the V1.0 module) corresponds to a current density of 0.1 A cm^{-2}, a module operating voltage of 4.02 V corresponds to a cell voltage of $0.67V_{cell}$ (equivalent to an electrochemical efficiency of 53% versus LHV). Further information regarding the relationship

between electrode performance and module performance, and system operation conditions can be found in a previous paper [8]. Industrial grade (99.95%) H_2 and N_2 are used. The air is scrubbed by passing it over soda lime (Sodasorb® from Grace). The gasses are fed at an over pressures of 3–5 10^3 Pa versus ambient. The module is operated using between 2 and 4 times stoichiometry (S) of air, the flow being regulated to ensure water management, a quasi-dead-ended hydrogen circuit (i.e. $1 - 1.1S$) and KOH is circulated at a rate of ca. 100 l h^{-1}/kW.

2.3. Description of the half-cell configuration

The half-cell set-up is presented in Fig. 2. The cell is installed in a test bench capable of running 10 cells simultaneously. Such test benchs allow for a rapid screening of materials without the requirement of complex gas and electrolyte distribution loop. The cells share a common electrolyte circuit. Each cell may be run independent of the other cells in the bench and furnished with a different flow of hydrogen, air or nitrogen. The cell is controlled electronically using a 48-positions multi-potentiostat from Arbin Instruments Inc. The software for data collection is MIST Pro provided by Arbin Inst. Inc.

In Fig. 2, the location of the reference electrode is not presented. Aluminium oxide fibres wicked with KOH are located near the working electrode and connected via an Al_2O_3 bridge to the H_2 reference electrode (from Gaskatel GmbH, Hydroflex HREF B01).

The hydrogen reference electrode is held at room temperature in a 6.6 M KOH solution (purchased from Brenntag, SA), whereas the working electrodes is held at 70 ± 2 °C. The potentials are quoted versus the reversible hydrogen reference potential at room temperature. An offset of 9 mV between the H_2 reference potential at 25 and 70 °C should be noted.

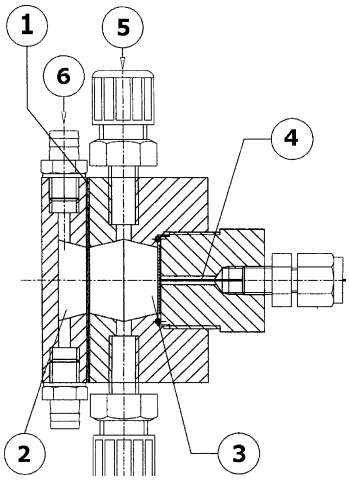

Fig. 2. Cross-section of the half-cell used for the electrochemical characterisation: 1, electrode; 2, gas chamber; 3, electrolyte chamber; 4, Pt counter electrode; 5, electrolyte outlet; 6, gas inlet. Not represented: reference electrode—an asbestos fibre is placed close to the electrode and connected to an external H_2 reference electrode (from Gaskatel GmbH) dipped in a solution 6.6 M KOH, 25 °C.

The 6.6 M KOH circulating electrolyte, is changed every 350 h. Gases are produced on-site using a H_2 electrolyser (from Packard) providing a 99.999%. H_2, N_2 generator (Nivox® from Permea) and a pure dry air compressor (from Atlas Copco with LXF superflow®). CO_2 is removed from the air by passing it over soda lime (Sodasorb® from Grace).

Gases flows in half-cell and single cell configuration (electrode surface: 4 cm^2) are fixed during the evaluation of the durability of the electrodes and are about 1 and 5 l h^{-1} for the H_2 and the air, respectively. The airflow is increased to >20 l h^{-1}, while the *I–E* curves are recorded. This high flow of air ($S > 10$) is used to limit the influence of air concentration gradient in the cell and ensure that the oxygen concentration in the cell is constant (i.e. 21%) regardless of current used (for current <0.7 A cm^2 and a 4 cm^2 sample).

For full cell testing, a similar electrochemical cell was used with slight modifications: the counter electrode is removed and replaced with the second electrode (the anode) using an identical frame for both gas chambers. A 17 mm distance separates the electrodes. No *IR* correction is made when presenting and discussing the result in the present paper. An external H_2 reference electrode is kept in the cell, close to the cathode, in order to separate the contribution in the losses of both electrodes. An additional voltmeter is connected between the reference and the cathode, is used to follow the evolution of the potential of the cathode. The subtraction of the cathode potential and the ionic resistance of the electrolyte chamber, from the cell voltage yields the polarisation curve for the anode.

2.4. Electrochemical test conditions

The cathode and anode, characterised in a 3-electrode cell configuration are polarised at 735 mV (for a current average current density output $j_{av.}$ of 0.18–0.22 A cm^{-2}) and 60 mV ($j_{av} = 0.15$–0.17 A cm^{-2}) versus RHE, respectively, for the evaluation of their durability. To determine their durability, the cathode and anode are maintained at constant polarisation in a 3-electrode half-cell configuration. Polarisation curves are recorded at regular intervals (i.e. once or twice a week) in order to monitor the evolution of electrode performance.

The degradation of the cathode is expressed considering the evolution of the current over time at 0.62 V versus RHE. Because the degradation at this potential is linear over time (t in h), one can follow the evolution of the current density, j (mA cm^{-2}) using the following equation:

$$j = \mathrm{De} \times t + j_{t0}$$

where De is the degradation factor in mA cm^{-2} h^{-1} and j_{t0} the extrapolation at $t = 0$. Moreover, the second reason driving the choice of this potential value is due to its sensitivity of the gas transport changes in the electrode. The explanation of the latter statement will be given later in the present paper.

Recently, a mathematical model was developed, which predicts the performance of a module from half-cell measurements of 4 cm^2 segments of cathode and anodes. This powerful tool also allows the polarisation losses of the electrode to be broken in to its components over the entire range of voltages [17]. The extension of such model to determine the durability of an AFC module from durability measurements made in half-cell is presently under development in our facilities [33].

The cell efficiency (or the electrochemical efficiency) is quoted in respect to the low heating value (LHV, 1.25 V) where V_{cell} is the voltage of the cell under working conditions.

$$\text{electrochemical efficiency (E.Eff.)} = \frac{V_{cell}}{1.25} \times 100$$

When considering modules, stacks and systems, one must also consider the issue of fuel usage. A fuel utilisation coefficient (μ_f) can be defined as

$$\mu_f = \frac{\text{mass of fuel reacted to yield current output}}{\text{mass of fuel input to cell}}$$

Combined this gives a total efficiency or the fuel cell efficiency (η), which is equal to

$$\text{total efficiency } (\eta) = \text{E.Eff.} \times \mu_f$$

3. Results and discussion

3.1. Latest improvement at Eident Energy

A full description of the 'Mark II" module design as well as the stack and system is given elsewhere [2,8]. Recently, new cathode and anode (called V1.1 electrodes) has been implemented into this module design. The modules containing these electrodes are called V1.1 modules. A polarisation curve is given in Fig. 3a, which compares the performance of the module containing the new V1.1 electrodes (Fig. 3b), with that of the previous version (Module V1.0 produced by ZeTek Power and its predecessors, Zevco and Elenco since 1990). The key parameters describing the current, V1.1 modules are summarised in Table 1. They are compared with the former Version V1.0 and with the version, in development V1.2. The material cost (or bill of material) based on a low production volume (50-units i.e. approx. 25 kW) is also compiled in Table 1. It can be seen that the use of these

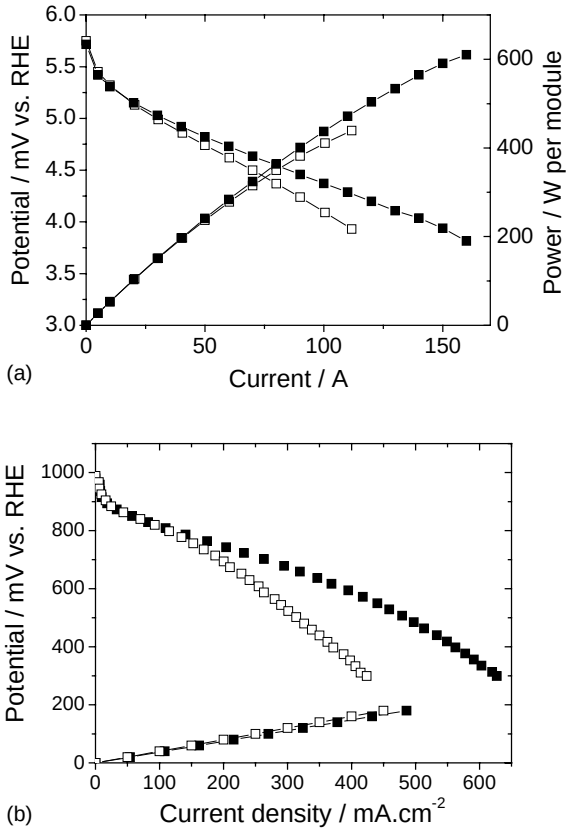

Fig. 3. Improvement of the performance of the Eident AFC technology due to newly introduced electrodes (V1.0 vs. V1.1). (a) Performance of EE AFC module—(□) Module V1.0 (June 2001): catalyst loading, 1.2 mg cm^{-2}; (■) Module V1.1 (April 2003): catalyst loading, 0.5–0.6 mg cm^{-2}. (b) Performance of the electrodes in a V1.1 module—(□) Version 1.0 (June 2001): catalyst loading, 0.6 and 0.65 mg cm^{-2} for the cathode and the anode, respectively; (■) Version 1.1 (April 2003): catalyst loading, 0.25–0.3 mg cm^{-2} for both the cathode and the anode.

Table 1
The evolution of the performance of Eident Energy AFC technology

	Platinum content		Power at 53% E.Eff. vs. LHV (W per module)	Lifetime[a] (h)	Power density[b]		Cost (€/kW)[c]
	Cathode (mg cm^{-2})	Anode (mg cm^{-2})			W l^{-1}	W kg^{-1}	
V1.0	0.64 ± 0.07	0.6–0.7	400	1000	52.6	85/67	908
V1.1	0.26 ± 0.02	0.26 ± 0.04	590	>2500	77.6	125/98	454
V1.2	0.26 ± 0.02	0.17 ± 0.02	590	>5000	77.6	125/98	430

[a] The definition of lifetime in the present document is given as being 30% current loss at nominal module voltage (4.0 V) (i.e. 670 mV per cell) [17]. An equivalent value for lifetime is obtained using the alternative definition of lifetime as a 10% decrease in operating voltage when the nominal current (defined as being that obtained at 0.67 V. cell at start of life), is maintained constant.

[b] Module dimension: 98 mm × 250 mm × 310 mm (=7.60 l), weight: 4.7/6.0 kg (excluding/including 1 l of electrolyte). Calculations made for a total efficiency of 51% vs. LHV.

[c] The cost is calculated as the bill of material at prices quoted on 25 May 2003, for volumes of material equivalent to a 50-unit production.

electrodes results in a significant increase of the module performance: the module performance increased by 35%, from 430 to 590 W, at the nominal operating voltage (4 V) (equivalent to E.Eff. = 53% versus LHV and η = 51% versus LHV).

At V_{cell} = 0.67 V (E.Eff. = 53% versus LHV), the specific power density of the V1.1 module is determined to be 0.16 W mg^{-1} Pt. The peak specific power is achieved at V_{cell} = 0.44 V (E.Eff. = 35% versus LHV). At peak power, the specific power density of the V1.1 module is 0.24 W mg^{-1} Pt.

The gain in module performance is due to a higher performance cathode. The limitation in power for the previous cathode is assigned to a low gas transport diffusion limitation through the active layer. No current density above 0.5 A cm^{-2} was attained with the previous cathode at high overpotentials when using air.

The air transport is drastically improved on the V1.1 cathodes compared to the V1.0 cathodes. As a consequence, at nominal voltage, the reaction rate is no longer limited by the flow of oxygen. Thus the module current produced at the nominal voltage (4.0 V, E.Eff. = 53% versus LHV) increases from 99–107 to 147 A (equivalent to an increase from 0.10 to 0.14 A cm^{-2} at 0.67 V per cell).

The components of the losses in the module polarisation curves (Fig. 3a) may be distinguished using a model [14,17]. Table 2 presents the kinetic, resistance and mass transport losses for the V1.0 and the newly introduced V1.1 versions for a standard 24-cell module (6 cells in series, 4 groups in parallel). The increased limiting current is proof of the improved air diffusion to the interface of the cathode in the V1.1 module (Fig. 3b). It is worthwhile mentioning the absence of dependence of the kinetic parameters, β (Tafel slope) and V_{rest} (rest voltage) on the precious metal loading in the electrodes. This quantifies the fact that, in the Version V1.1 cathodes, the catalysts particles are simply made accessible to participate in the electrochemical reactions. In other words, there was a higher degree of catalyst redundancy in the V1.0 electrodes: a larger proportion of the catalysts was in inappropriate location: either in a non-wetted area of the electrode or were rendered useless due to the limited amount of air dissolved in the 3-phase interface.

The increase in cathode performance is also due to a decrease in the gradient of the linear part of the *V–I* curves of ca. 30%. The use of the model [14,17] demonstrates that, this improvement is related to a lower influence of the air mass transport limitation as opposed to an increase of the electronic conductivity of the electrodes or any change in the electrode thickness. The use of the electrochemical impedance spectroscopy technique will allow us to confirm this, and also determine the component of ionic and electronic conductivity.

The increase in diffusion limit also leads to an improvement of the peak power of the V1.1 module (Fig. 3a). A peak power of 0.8 kW is achieved at 2.6 V (i.e. 35% E.Eff. versus LHV). The V1.0 yields a maximum power of 0.5 kW. This feature is important for fluctuating power demands.

Interestingly, this increase in performance is accompanied with a decrease of the platinum content to a value of 0.26 mg cm^{-2} on each electrode. This represents a reduction of a factor 2–3 times in both the anode and cathode over the value in the V1.0 electrodes. This apparent paradox can be resolved as the improved electrode structure results in a lower degree of catalyst redundancy in both anode and cathode and, in the case of the cathode, improved gas access to the active catalytic sites, compared to the previous V1.0 electrodes. The breakdown of the losses at a constant electrochemical efficiency (53% versus LHV) calculated according to the model presented in Ref. [17], shows that the limitation due to the air diffusion at a cell voltage of 0.67 V is decreased from 5.2 to 2.2% for the new version of the module [33]. Optimising the utilisation of the Pt on the electrodes obviously results in a decrease of the cost of the AFC technology.

As shown in Fig. 3b, the V1.0 and V1.1 anodes have equivalent performance but the latter have a precious metal loading half that of their predecessors (i.e. currently 0.26 ± 0.04 mg cm^{-2}). Furthermore, anodes with precious metals loadings <0.15 mg cm^{-2} are currently under investigation. Increasing noble-metal participation in the reaction will yield little gain in performance since the HOR is a fast reaction and the overpotential η_a observed in the current density of interest (i.e. 0.15 A cm^{-2}) is low (i.e. η_a < 60 mV). Indeed, it is possible to dilute the carbon modified with precious metals via the inclusion of up to 50% volume of an inert, catalyst-free, highly conductive carbon without any detrimental effect for performance. In fact, it is probable that the increase polarisation loss is countered by an equivalent decrease in the electronic and ionic resistance due to improved electrode structure.

The values for fuel cell performance and catalyst loading quoted here are similar to those recently reported by Han et al. for an AFC application [34]. For a 0.3 mg cm^{-2} platinum

Table 2
Kinetic parameters calculated for a 24-cell module (6 series and 4 groups in parallel)

	Cell voltage		Tafel slope, β (V per decade)	Ohmic resistance		Limiting current (A cm^{-2})
	Rest (V_{rest}/V)	Intercept[a] (V_o/V)		Total (Ω)	Single cell (Ω cm^{-2})	
V1.0	0.956	0.899	0.073	0.0132	2.35	0.2–0.25
V1.1	0.953	0.879	0.070	0.0091	1.55	0.4–0.5

[a] V_o is the intercept with the *y*-axis (of the linear part of the *V–I* curve) following the equation: $V = V_o - R_i$, R is the total resistance for the module.

load on both electrode the 5 cm^2 cell was providing a power output of 77 mW cm^{-2} at 48% E.Eff. versus LHV while at the module level, the present version developed in the company is 100 mW cm^{-2} at 53% E.Eff. versus LHV. Moreover, identical precious metal content is reported elsewhere as being the state-of-the-art catalyst content for PEMFC using the commercially available Pt-supported carbons [35,36].

3.2. Ageing in alkaline fuel cell

3.2.1. Module ageing

Fig. 4 presents the evolution of the performance of a V1.0 module running under pure oxygen and pure hydrogen. The time axis is the number of hours the module is in the test stand. It should be noted that, in the case of discontinuous operation, the module would only be operated a fraction of that time. The operating hours only equal to the hours in the test stand in the case of continuous operation. During the first part of the experimental characterisation, the module was run discontinuously over a period of 4000 h (○). In discontinuous operation the module is operated 7 h each working day. This means that during this initial period the start-up and shutdown procedure was performed more than 160 times. During the idle time, the module is stored at room temperature with both gas chambers filled with N_2 and electrolyte chamber kept filled with static KOH. In the second part of the curve, the module was characterised under continuous 24 h operation (●). During the weekend period, the module was idle. One can here conclude that the deterioration of the performance is independent of the continuous or discontinuous testing operation: the evolution of module performance is identical when the module is operated 35 or 120 h a week (i.e. a factor of 4 in number of operating hours). Indeed it appears to be purely a function of the time the module is kept under a static pressure of KOH. If electrochemical corrosion were the key source of module deterioration, one would expect the deterioration to be a function of operating hours. This implies that the module is suffering from physical or chemical degradation.

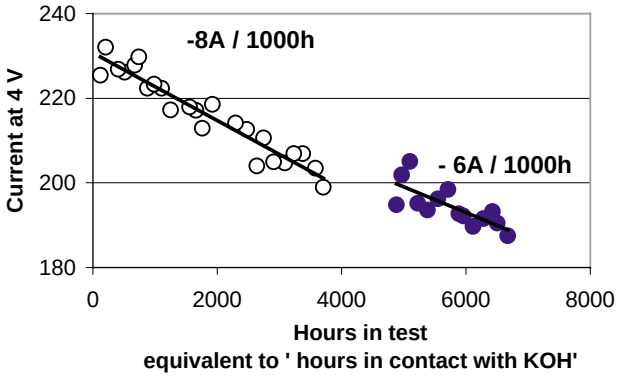

Fig. 4. Evolution of the performance of a module as a function of the time in test i.e. time in contact with the electrolyte 6.6 M KOH. Operating conditions: pure oxygen, pure hydrogen. (○) Module is operating following the time basis 7/24 5/7 (discontinuous operation). Experimental slope for degradation: 8.0 ± 0.5 A/1000 h, R^2 = 96%. (●) Module is operating continuously i.e. 24/24 5/7. Experimental slope for degradation: 6.0 ± 1.5 A/1000 h, R^2 = 75%.

A gap of 1000 h separates the two operation regimes. During this period, the module was removed from the test stand, drained of KOH, and stored under air at room temperature. No degradation occurs during this period. Indeed modules have been stored in this manner for many years (>5) and no change in performance is observed on restarting the module after this time. During this storage-period the electrodes still are wetted with KOH, and may contain droplets of KOH. If the degradation were due to a chemical reaction with KOH, this would continue during this storage and one would expect a continual degradation to occur, during storage. This implies that the degradation process must be due to a physical ageing. Furthermore, we note that the degradation of the module performance is directly proportional to the time the module is in contact with a static pressure of KOH.

It is clear that one should drain the KOH out of the stack and into a vessel, when the module is not operating. During start-up, the KOH may be rapidly pumped into the module in 30 s or, in the case of a KOH vessel, which is above the stack, simply flowed into the stack using gravity. An additional advantage of storage in this manner is that one can be sure that the gas chambers remain liquid-free during storage, this allows for a more rapid start-up procedure as the gas chambers do not need to be blown out with nitrogen prior to start-up.

3.2.2. Electrode ageing

Insight into the origins of the module may be achieved by the study of durability measurements performed using the full cell set-up as described in the experimental section. The full cell set-up and the electrochemical testing conditions mimic those used when testing modules. The cell was kept polarised at 0.08 A cm^{-2}, 24 h a day, 7 days a week. Polarisation curves were recorded after performance stabilisation (24 h) and then after 100, 250 and 480 h. The results are shown in Fig. 5a. Whilst the polarisation curves for the full cell are being recorded, the evolution of the cathode potential is also recorded versus the H_2 reference electrode using a voltmeter. This data, displayed in Fig. 5b, allows the polarisation curve for the anode to be deduced (Fig. 5c). The *I–E* curve for the anode is here not corrected of the ohmic losses due to the electrolyte chamber.

No change of the anode polarisation is observed over the considered time scale and from these three figures, it is clearly observed that the full cell degradation is coming solely from the cathode. The similarity of the evolution of the module and the full cell results allow us to eliminate the possibility that degradation is due to module assembly and operation conditions.

A closer observation of the cathode polarisation curves shows that the evolution in performance is primarily due to changes in the diffusion limit. The activation and resistance

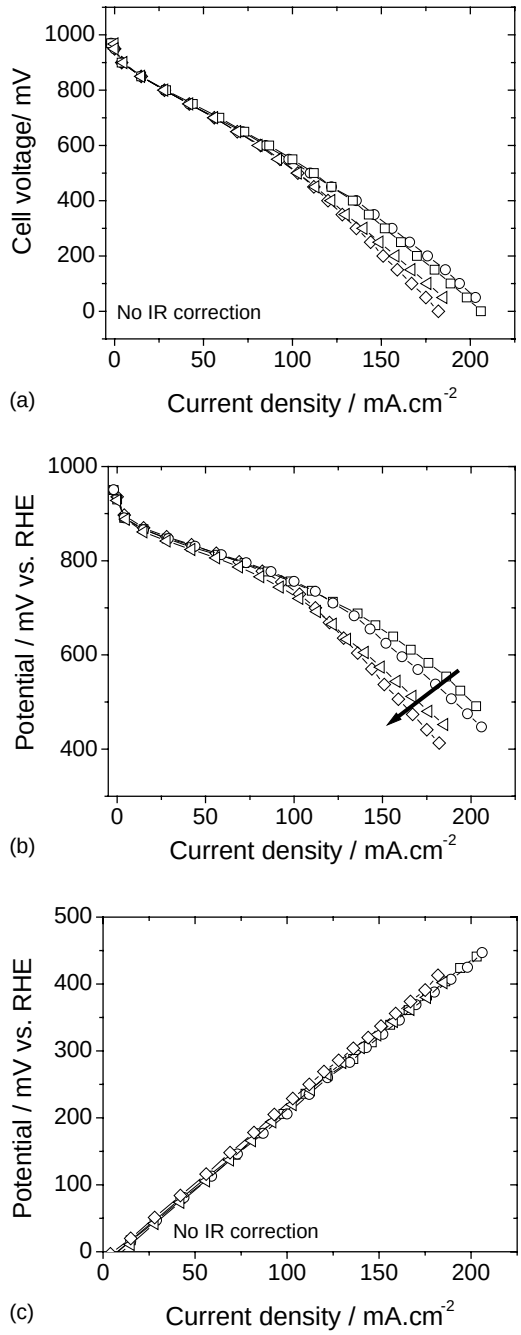

Fig. 5. Evolution of the performance of a 4 cm^2 single cell (V.1.0) as a function of the time: (a) under continuous operation at constant voltage (0.6 V), electrolyte: 6.6 KOH, 70 °C, gases: air (1.05 10^5 Pa) and H_2 (1.05 10^5 Pa). The contribution of each electrode vs. RHE is presented in graphs (b) and (c) for the cathode and the anode, respectively: day 1 (□), day 4 (○), day 11 (◁), day 20 (◇).

of the cathode polarisation curve remain constant. The kinetics parameters (open circuit potential OCP, Tafel slope and E_0 [24]) and the polarisation resistance of the cathode remain constant over the duration of the experiment, this is also observed when investigated over a period of 1200 h in the half-cell configuration at 0.15 A cm^{-2} (Fig. 6). The slight drift of the OCP is attributed to a partial (reversible) oxida-

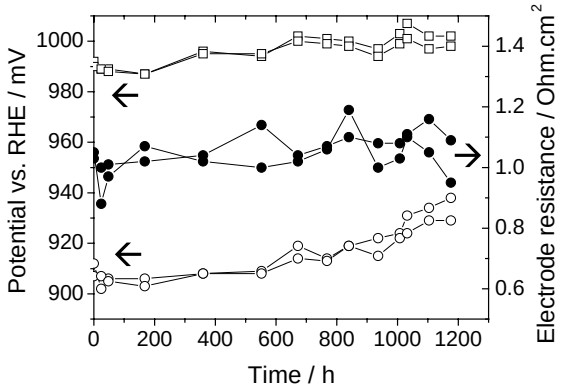

Fig. 6. Evolution of the cathode kinetic parameters and of the electrode resistance R (Ω cm^2) over operating time in half-cell configuration. Electrode resistance (●), rest potential (□), extrapolated potential (○) (E_0 from $E = E_0 - R_i$ [24]). Electrodes: cathodes V1.0.

tion of the platinum particles. The initial values for the OCP and E_0 can be recovered when appropriate electrochemical activation is carried on (see Section 3.2.3).

Any change in the quantity, and activity of the catalyst would be observed in the activation part of the polarisation curve at low current densities. The fact that the activation component of the curve remains constant indicates that no decrease of the electroactivity of the catalytic sites is happening in the cathode over this time range. Indeed the Tafel slope β (overvoltage $\propto \log j$). β = 70–80 mV per decade over the experiment remains also unchanged. This eliminates the possibility that ageing is due to such phenomena as dissolution, corrosion, sintering, poisoning or catalyst deactivation.

The limitation due to gas transport inside the catalytic layer is observed at high current densities. Indeed one knows that the limitation is due to air transport, as opposed to e.g. ions or water, as replacing the air by pure oxygen moves the diffusion limit to higher values. The diffusion limiting current is decreasing over time to lower current density values. This is due to a more difficult gas access to the reaction sites i.e. gas pores are becoming blocked. Concurrently, we observe a slight increase of the cell capacitance due to a greater surface of electrode covered in liquid. This is indicative that the cathode is getting wetted over time. The evidence for product build-up (OH^- and HO_2^- and/or reactant depletion (H_2O)) in the pores was also observed elsewhere with Pt 10% supported on carbon [28]. The build up of liquid electrolyte, in the gas pores, due to the gradual wetting of the cathode, may be considered to be hindering the efficient diffusion of O_2 through this electrolyte layer. One can infer that it is this liquid build-up, which is filling and blocking the gas pores.

An additional evidence of the flooding of the cathodes is presented in Fig. 7, where with an appropriate chemical treatment, the excess of KOH is removed from the surface of the electrode and the cathode recovers its initial performance. This clearly proves the absence for any irreversible

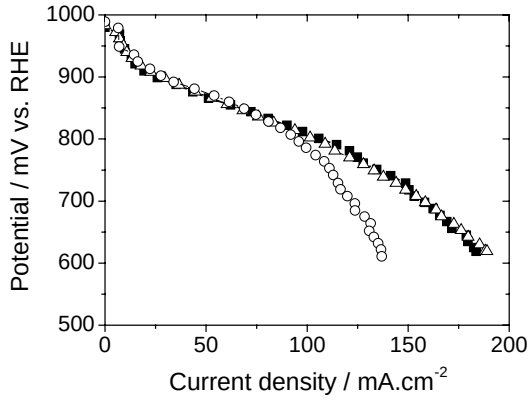

Fig. 7. Recovering the electroactivity of a cathode after 850 h continuous running in half-cell configuration. *I–E* curves: (■) initial performance ($t = 24$ h), (○) performance after 850 h and (△) performance after 850 h and chemical treatment.

degradation process. This is consistent with the work of Lamminen et al. [37] who also attribute the decay of performance to a rapid flooding of the electrodes.

Kordesch and co-workers have also observed the flooding of the cathode but in their experiments they assign it to be a result of carbon corrosion [19]. The presence of inorganic impurities in the carbon has been shown to play a significant role in carbon corrosion and to be one of the reasons for the electrode degradation [13]. Consequently, the choice of the carbon (its purity, pore structure and hydrophobic–hydrophilic behaviour) is critical to the activity and to the stability of the electrode. The carbon materials available today have a low level of impurities. Surface analysis e.g. X-ray photoelectron spectroscopy (XPS) of the carbons used in the EE electrodes do not detect the presence of minerals (i.e. Mg, Na and Ca) or sulphur [38]. These carbons do not appear to suffer from electrolyte attacks and the effect of carbon corrosion on the performance of the electrode, typified by an increase in the ohmic resistance component of the polarisation curve as a function of the number of operating hours, is not observed in the present electrodes over this time frame.

3.2.3. Cathode degradation: temperature/operating conditions dependence

As the cathode flooding is appearing to be the main parameter driving the degradation of the module performance, it was of interest to evaluate the influence of the operating conditions (thermal, Table 3 and electrochemical conditions) and thus to confirm the interpretation presented in Section 3.2.2. This was simulated considering the evolution of the performance of cathodes in a 3-electrode cell configuration.

In Table 3, two similar samples of V1.1 cathode were polarised continuously at 0.73 V versus RHE firstly at 70 °C (from 0 to 500 h) and then at room temperature (from 500 to 700 h). The flooding of the electrodes was evaluated by

Table 3
Degradation of the cathode as a function of the operating temperature

Operating conditions	Cathode degradation measured at 0.62 V vs. RHE ($\mu A\,cm^{-2}\,h^{-1}$)	
	Sample 1	Sample 2
70 °C/from 0 to 500 h	54	37
Followed by 20 °C/from 500 to 700 h	46	51

recording the evolution of the current obtained at 0.62 V versus RHE, this relates to the evolution of the limiting current overtime. Although a certain dispersion of the values is observed, one notices that the degradation, the flooding, is not temperature-dependent. The rate of flooding (measured as the decay of the current in $\mu A\,cm^{-2}\,h^{-1}$ at 0.62 V versus RHE), due to KOH penetration, is the same if the cathode is polarised at 0.73 V versus RHE at 70 °C (43 $\mu A\,cm^{-2}\,h^{-1}$ for an average j output >0.1 $A\,cm^{-2}$) or left standing in contact with a static pressure of KOH at room temperature (56 $\mu A\,cm^{-2}\,h^{-1}$ for a zero current output). Additionally, the absence of real influence of the electrochemical conditions on the rate of cathode deterioration confirms the results in Fig. 4: the rate of module and electrode deterioration is independent on electrode operation. This result allows us to determine that the method of flooding is not from any electrochemical processes (i.e. creep) or chemical reaction and chemical degradation, but simply due to a physical wetting phenomenon in which the pressure of the static KOH (0.5–1.0 10^4 Pa over ambient) forces the KOH into the dry pores.

3.2.4. Reversible ageing due to the catalyst oxidation

A second source of ageing has been recently observed while evaluating the cathodes durability; this reversible phenomenon is a function of the polarisation potentials of the electrode. The cathodes were successively polarised at different potentials, respectively, 0.8, 0.73 and 0.65 V versus RHE and the loss of the current overtime at those different potentials evaluated in the half-cell configuration. The results are synthesised in Table 4. The same experiment has been carried out using a full cell set-up (in order to mimic the experimental conditions imposed in modules) where the cell was polarised at 0.6 V (av. j: 0.1 $A\,cm^{-2}$), then 0.8 V (av. j: 0.03 $A\,cm^{-2}$) and finally at 0.3 V (av. j: 0.21 $A\,cm^{-2}$).

The results demonstrate an inverse relationship between the depth of polarisation and the degradation. Somewhat

Table 4
Degradation of the cathode as a function of the depth of load in the half-cell configuration

Experiment time scale (h)	Potential set to the cathode (V vs. RHE)	Average J output ($A\,cm^{-2}$)	Current loss ($\mu A\,cm^{-2}\,h^{-1}$)
0–912	0.73	0.18–0.19	33
912–1248	0.65	0.25	26
1248–1752	0.8	0.08	48

surprisingly, the greater the polarisation of the cathode i.e. the lower the potential of the cathode/lower the cell voltage (i.e. higher the load); the lower the degradation of the cathode/cell. This is the opposite of what one would expect for the corrosion of the electrode.

In the present case, one can interpret the degradation as being due to the partial oxidation of Pt catalysts to form $Pt(OH)_2$ or/and PtOH [27] at the cathode at the 3-phase interface. These species are not electroactive towards the ORR and the rate of their formation is non-negligible at potentials above 0.8 V versus RHE [23,39]. The quantity of oxides present has been showed to be three times larger at 0.9 V than at 0.7 V versus RHE [27]. The reduction of the Pt hydroxides/oxides back to the electroactive Pt metal occurs when the cell/the cathode is polarised at high overvoltages/potentials and thus the initial performances are recovered. Such behaviour is similar to observations recently reported for a PEM cell and the authors also report that the performance maybe recovered simply by shutting down the cell and restarting it [40].

The technical consequence of such behaviour at the module/stack/system level during continuous polarisation would be the possible need for reactivation procedure. A punctual dynamic load or deeper load may be needed in order to 'reactivate' the surface of the electrode via the reduction of the Pt particles. This will be investigated shortly at the module/stack level. However, for long polarisation time, one can also expect the flooding to overshadow this reversible effect.

4. Conclusion—perspectives

The most recent information on the evolution of the performance of the AFC technology at Eident Energy has been presented. New materials have been introduced in the commercial EE module, achieving a decrease of the precious metal loading to $<0.6\,mg\,cm^{-2}$ (ca. 0.25–0.3 $mg\,cm^{-2}$ on each electrode). This loading and cost reduction is achieved via an improvement in the electrode structure and a resultant reduction in catalyst redundancy. At the same time, a 50% increase of the performance was achieved to $0.137\,A\,cm^{-2}$ at 0.67 V per cell. This is equivalent to 147 A at 4 V at total efficiency of 51% versus LHV. The improvement is due to the large increase in the diffusion of air inside the cathode.

The durability has been also investigated from the half-cell level to the module scale over the first thousand hours. Degradation is shown to be independent of electrode operation and operating temperature, and only a function of the time that a cathode is kept in contact with a static pressure of KOH. Sources of degradation were clearly identified. They originate from a slow but constant physical flooding of the cathodes. Consequently, the diffusion of air to the active sites is made more difficult and the limiting current due to air diffusion is reduced. Fortunately, it appeared to us that the performance could be recovered. Efforts are now being devoted to the improvement of cathode stability. From the results presented in this paper several strategies are being pursued in order to stop, or to dramatically reduce, the rate of flooding. Some have been already initiated and are as simple as modifying the operating procedure of the stack to minimise the time during which a module is inoperative and has a static pressure of KOH applied. The group is now also screening several alternative preparation methods in which the cathode is made more resilient to the effect of flooding. These include improving the waterproofing of the electrode via the use of more hydrophobic carbons, the optimisation of the quantity of PTFE, the utilisation of PTFE suspension for an intimate waterproofing of the carbon pores, via appropriate heat treatments of the intermediates or the finished electrodes. The first results are encouraging, demonstrating improved cathode stability over 2800 h at a cell current output in excess of $0.15\,A\,cm^{-2}$ at 0.67 V. The degradation rate is ca. 5–10 mV/1000 h and 20 mV/1000 h at 0.1 and $0.2\,A\,cm^{-2}$, respectively. The results will be described shortly in a communication, which is currently in preparation.

The observation of the degradation processes need to be extended to longer periods under electrical load. At these longer timescales (>5000 h) one might expect to observe the corrosion of the electrodes (both anode and cathode) as well as a possible degradation of the PTFE.

References

[1] http://www.h2fc.com/companies.html (last accessed November 2003).
[2] http://www.independentpower.biz (last accessed November 2003).
[3] K. Kordesch, Proceedings of the First Olle Lindström Symposium on Renewable Energy, Fuel Cells, November 19, 1997.
[4] K. Kordesch, J. Gsellmann, M. Cifrain, S. Voss, V. Hacker, R.R. Aronson, C. Fabjan, T. Hejze, J. Daniel-Ivad, J. Power Sources 80 (1999) 190.
[5] G.F. McLean, T. Niet, S. Prince-Richard, N. Djilali, Int. J. Hydrogen Energy 27 (2002) 507.
[6] W.M. Vogelm, J.T. Lundquist, J. Electrochem. Soc. 117 (1970) 1512.
[7] K. Kinoshita, Electrochemical Oxygen Technology, Wiley, New York, 1992, pp. 37–40.
[8] E. De Geeter, M. Mangan, S. Spaepen, W. Stinissen, G. Vennekens, J. Power Sources 80 (1999) 207.
[9] K. Kinoshita, Electrochemical Oxygen Technology, Wiley, New York, 1992, p. 188.
[10] D.R. Lide (Ed.), Handbook of Chemistry and Physics, 81st ed., CRC Press, Boca Raton, FL, 2000–2001, pp. 8–103.
[11] E. Gülzow, J. Power Sources 61 (1996) 99.
[12] O. Lindstrom, Proceedings of the Fuel Cell Seminar, San Diego, CA, 1994, pp. 297–298.
[13] K. Kordesch, G. Simader, Fuel Cells and their Applications, Wiley, New York, 1996, p. 72.
[14] J.H. Miners, Eident Energy, Internal Report, May 2003.
[15] D.R. Sena, E.R. Gonzalez, E.A. Ticianelli, Electrochim. Acta 37 (1992) 1855.
[16] A.J. Appleby, Energy 11 (1986) 95.
[17] T. Burchardt, P. Gouérec, E. Sanchez-Cortezon, Z. Karichev, J.H. Miners, Fuel 81 (2002) 2151.
[18] Fuel Cell Power System Performance: Performance Test Codes ASME PTC 50-2002, American Society of Mechanical Engineers, 2002.

[19] K. Tomantschger, R. Findlay, M. Hanson, K. Kordesch, S. Srinivasan, J. Power Sources 39 (1992) 21–41.
[20] J.M.J. Blomen, M.N. Mugerqa (Eds.), Fuel Cells Systems, Plenum Press, New York, 1993, p. 251.
[21] Elenco NV, Fuel Cell brochure, Dessel, Belgium, 1990.
[22] J.O.M. Bockris, A.J. Appleby, Energy 11 (1986) 95.
[23] M. Pourbaix, Atlas of Electrochemical Equilibria in Aqueous Solutions, 1974.
[24] J. Saint-Pierre, D.P. Wilkinson, S. Knights, M. Bos, J. New Mater. Electrochem. Syst. 3 (2000) 99.
[25] A. Blanchart, J. Lichtenberg, E. Rousseau, W. Stinissen, G. Van Bogaert, Fuel Cell Work for Hermes, April–October 1988 (Final Report, 1989).
[26] http://ww/w.avistalabs.com (last accessed November 2003).
[27] K.A. Striebel, F.R. MacLarnon, E.J. Cairns, J. Electrochem. Soc. 137 (1990) 3351.
[28] K.A. Striebel, F.R. MacLarnon, E.J. Cairns, J. Electrochem. Soc. 137 (1990) 3360.
[29] E. Sanchez-Cortezon, Ph.D. Dissertation, Technische Universität Berlin, Germany, 2002.
[30] X. Li, K. Horita, Carbon 38 (2000) 133.
[31] Y. Kiros, S. Schwartz, J. Power Sources 87 (2000) 101.
[32] Y. Kiros, C. Myren, S. Schwartz, A. Sampathrajan, M. Ramanathan, Int. J. Hydrogen Energy 24 (1999) 549.
[33] P. Gouérec, E. Sanchez-Cortezon, J.H. Miners, in preparation.
[34] E. Han, I. Eroğlu, L. Türker, Int. J. Hydrogen Energy 25 (2000) 157.
[35] Z. Qi, A. Kaufman, J. Power Sources 113 (2003) 37.
[36] H.A. Gasteiger, S.S. Kocha, R. Makharia, M.F. Mathia, T.E. Moylan, S.G. Yan, Proceedings of the 203rd ECS Meeting, Paris, France, April 27–May 2, 2003.
[37] J. Lamminen, J. Kivisaari, M.J. Lapinen, M. Viitanen, J. Vuorisalo, J. Electrochem. Soc. 138 (1991) 905.
[38] Zevco Belgium BvBa, Final Technical Report, European Program (Brite-EuRam III), April 1998–December 1999.
[39] V. Srinivasamurthi, R.C. Urian, S. Mukerjee, Proceedings of the 203rd ECS Meeting, Paris, April 28–May 2, 2003.
[40] T.D. Jarvi, T.W. Patterson Jr., N.E. Cipollini, J.B. Hertzberg, M.L. Perry, Proceedings of the 203rd ECS Meeting, Paris, April 28–May 2, 2003.